CHAPTER

Actuation for robot-aided rehabilitation: Design and control strategies

4

Lorenzo Masia, Michele Xiloyannis, Dinh Binh Khanh, Antuvan Chris Wilson, Sara Contu, Kim Giovanni Yongtae

Nanyang Technological University, Singapore

INTRODUCTION

The importance of the human brain in controlling human movements scarcely needs to be argued. Even a slight damage of nervous system can severely hamper one's ability in performing simple yet crucial activities of daily living. Stroke is the most prominent cause of neurological disorder [1] and is a leading cause of long-term impairment [2]. The incidence of stroke has been shown to increase with age, and as the lifetime expectancy rises, its prevalence and impact on society are deemed to grow. Various strategies have been explored to improve recovery after stroke, and so far, repetitively performing isolated and functional [3] movements in the acute phase of recovery has produced the best outcomes. Robotic devices can relieve the therapists from the demanding task of manually assisting the patient and have shown encouraging results, comparable with the ones achieved with traditional therapy while allowing greater patient compliance and a systematic monitoring of the patient's performance.

In order to be effective, rehabilitation robots need to interact with humans in a gentle but decisive manner. The actuation stage, the overall architecture, and the control strategy, among other factors, play a fundamental role in ensuring the efficacy of the rehabilitation procedure. In this chapter, we provide the reader with an overview of the actuators used for robotic rehabilitation and describe the control strategies used for modulating the interaction with the patient, namely, impedance and admittance control.

Section "Robot Architectures and Actuators" lists the most common choices for the motors, touching on the advantages and drawbacks of pneumatic, hydraulic, and electric motors. The difference between end-effector robots and exoskeletons is defined, with examples from some of the most popular commercially available and researched devices. Sections "Control Strategies" and "Friction and Backlash Compensation" present, respectively, the high- and low-level control strategies used in rehabilitation robotics, emphasizing the difference between traditional servo-controlled robots for industrial tasks and devices that need to interact and exchange

Rehabilitation Robotics. https://doi.org/10.1016/B978-0-12-811995-2.00003-5

information with and assist movement of human beings. Section "Control Strategies" deals with understanding the user's performance and modulating the level of assistance, in terms of the impedance at the human-robot interface; Section "Friction and Backlash Compensation" presents a brief review of the models used for compensating nonlinearities deriving from the robot's architecture, such as friction and backlash, whose effect could otherwise compromise the performance and stability of the controller. Finally, we focus on the mechanical design choices of the actuation stage of a robot for rehabilitation, dealing with the challenging trade-off between high force delivery and backdrivability and its implications for implementing an effective control strategy.

ROBOT ARCHITECTURES AND ACTUATORS

Rehabilitation robots can be broadly classified in two groups based on the nature of their mechanical attachment to the human body: end-effector robots (examples shown in Fig. 1) and exoskeletons (examples shown in Fig. 2) [6]. In the case of an end-effector robot [5,7,8], the human-robot interface is generally attached at the distal part of the body and does not constrain the kinematics of the human joints but applies a force in the Cartesian space. These devices are much simpler in construction and easier to control when compared with the exoskeleton-type robots.

Exoskeletons [9,10], on the other hand, wrap around the human body, acting as an external, parallel skeletal structure and allow for independent control of each individual joint of their wearer. The complexity of the structure increases with the number of degrees of freedom (DoF) to be controlled. One of the key issues with these types of robots is the misalignment between the human joint and robot's counterpart, which leads to undesired interaction forces on the human limb, upsetting the natural smoothness of human kinematics. Recent research has focused on design methodologies to compensate for this issue, but these often result in a more complex and bulky kinematic structure [11].

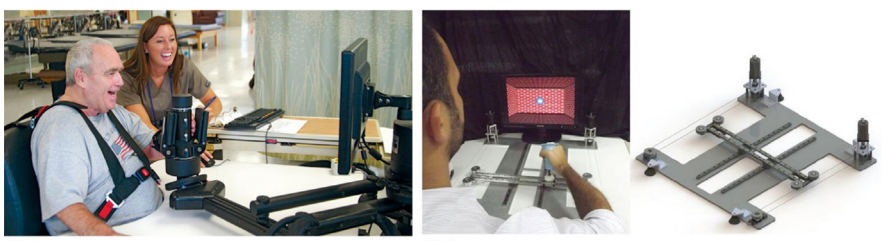

FIG. 1

End-effector robots for rehabilitation. (A) MIT-Manus [4] (InMotion ARM, MA, United States) is a serial link end-effector-based robot. (B) H-Man [5] is a cable-driven planar end-effector device.

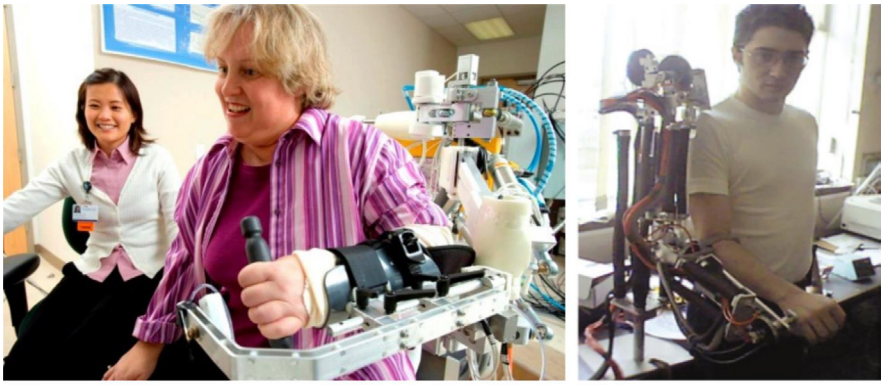

FIG. 2

Pneumatically actuated exoskeletons for rehabilitation. (A) Pneu-WREX [13], a four DoF pneumatically controlled device. (B) Salford Arm Rehabilitation Exoskeleton based on PAMs [14].

In both the cases mentioned above, the actuation unit can be placed either distally or proximally, the position of the motors affecting the dynamics of the system. Placing the actuators directly at the joint level strategy avoids the need of a transmission mechanism but increases the inertia of the moving parts, thereby making the control less transparent and more power-consuming. In the case where the actuators are placed proximally [12], a transmission mechanism is required to transmit the torque at the distal location. This helps to reduce the inertia at the joint but introduces the challenge of compensating for the nonlinear dynamics that may arise in the transmission, such as hysteresis and friction.

A wide variety of actuation technologies have been used to develop robotic devices meant for rehabilitation. These can be classified according to the nature of the energy source used to generate mechanical power: hydraulic, pneumatic, and electric motors are among the most common.

In the past, hydraulic actuators have been used for developing rehabilitation robots (examples are shown in Fig. 2), but due to the inherent nature of being bulky, noisy, and prone to fluid leakages, their usage has been declining. Pneumatic actuators in comparison with hydraulic actuators are lighter and quieter but still challenging to embed in a portable system since the compressor unit is quite heavy [15,16]. However, they provide a higher power-to-weight ratio and lower impedance compared with their electric counterpart. Pneumatic artificial muscles (PAMs), based on a bioinspired working principle, have more recently been utilized for developing rehabilitation devices due to their lightweight characteristics and inherent compliant nature [14]. PAMs consist of an inflatable bladder that increases in diameter and shortens in length as compressed air is pumped into them. These pneumatic actuators work only in contraction (unidirectional); therefore, at least two units are required to perform agonist-antagonist motion.

Electric actuators are the most widely used solution mainly because of their high power density and ease of use. High gear reduction can be used to increase the torque output but at the cost of increasing the mechanical impedance of the system, thereby reducing the backdrivability of the system. It is highly desirable to have systems that are backdrivable, for safer interactions between humans and robots and in implementing control strategies, such as impedance control, that are fundamental when assisting human motion.

Simply placing an elastic element in series with an electric motor makes it possible to lower the impedance levels in the system and achieve a more accurate force control. The main advantages of using series elastic actuators (SEAs) are securing safety and improved performance of force (torque) control bandwidth [17]. Indirect force/torque control can also be implemented on stiff actuators with impedance control; however, the main difference between the compliance of SEA and impedance control of stiff actuators is the intrinsic safety [18] of the former, which still applies in the case of control failure.

The main disadvantages of using SEAs are the need of extra components and a deterioration of position control performance. The position control bandwidth is normally lower than that of conventional actuators because the input command of SEA is force/torque [19]. Using SEA in rehabilitation scenarios is a good option because many rehabilitation tasks require precise force/torque control and intrinsic safety. Examples of SEA-based rehabilitation robots are the Lopes [20] and Lokomat [21].

At the current state of the art, most of the implementations make use of traditional electric motors with the addition of a compliant element and/or a controller that modulates the interaction forces with the subject. The rest of the chapter will thus focus on control strategies typically used with electric motors.

CONTROL STRATEGIES

The complex interaction and flow of information occurring between a human being and a robot during a rehabilitation session requires to be addressed via control paradigms different from the traditional servo systems [13,22]. Aside from stability, there are two fundamental requirements that need to be considered, namely, the controller needs to understand the subject's intentions and ensure correct human movements.

In the initial stages of recovery, when voluntary movement is absent or not trustworthy, traditional control methods, defining a desired trajectory/force profile and treating the human interactions as disturbances, may be applied. However, when the subject starts to regain the ability to move, the robot needs to be complementing such actions rather than rejecting or hindering them, assisting the user when needed [22].

Such paradigm, known as assist-as-needed, requires controlling the interaction at the human-robot interface rather than the forces or the position of the device, to both understand the user's intentions and change the behavior of the robot from a very stiff to a compliant interaction.

A conceptual control diagram on the interaction between robots for rehabilitation and assistance and a human being is shown in Fig. 3A [23]. The motion control in a human body can be simplified as a feedback loop, where the brain plays the role of controlling human motions. The brain controls the muscles to follow an arbitrary desired motion X_d. The control output u_h generated by the brain is the motor control signal, sent to the muscles to produce a joint torque F. The input (i.e., human motion intention) to the robot can be extracted from the human-robot interface,

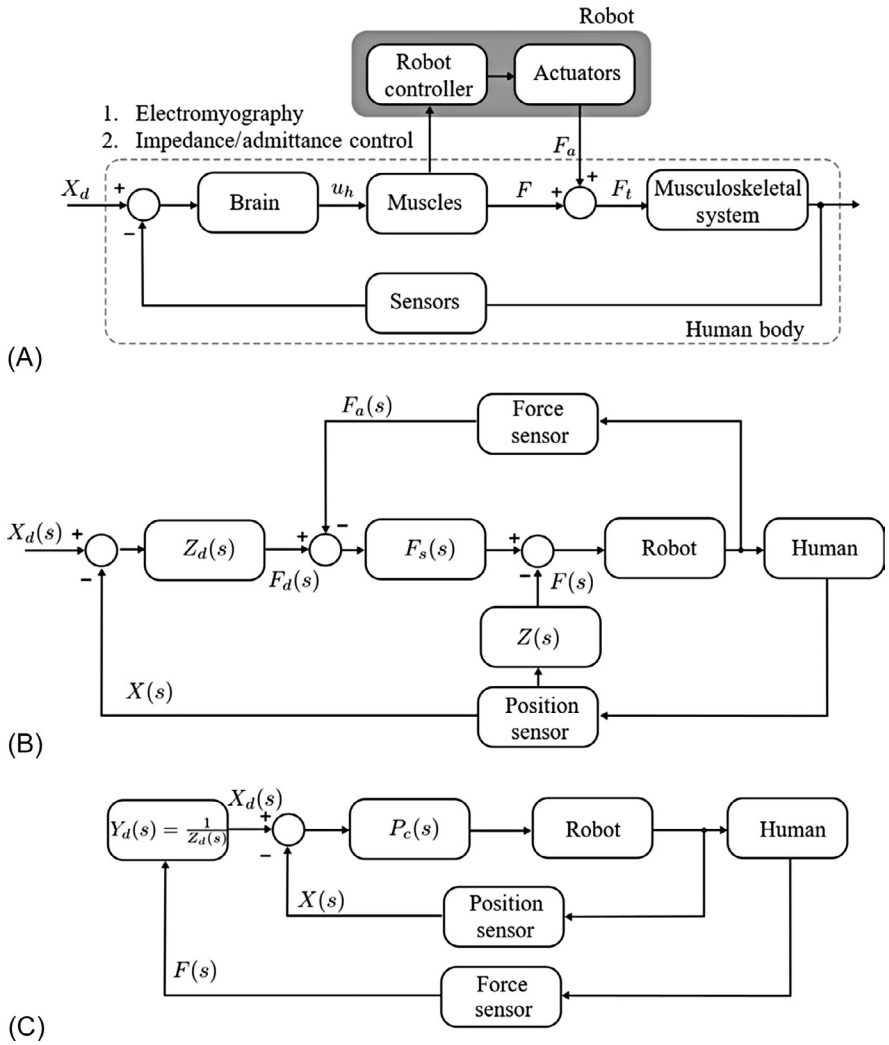

FIG. 3

(A) Human-robot interaction control system. (B) Closed-loop impedance controller. (C) Admittance controller.

through force sensors or muscle-related signals. The robot's controller can then command the actuators to generate an assistive torque (F_a) accordingly, delivered to the musculoskeletal system. In other words, the human body is actuated by the sum of a muscular torque F and an additional assistive torque F_a, complementing its movements. Sensing technologies for detecting the human motion play a vital role, and identifying the exact human intention in a robust and effective way is still an open challenge.

A common sensing method is surface electromyography (sEMG); it is known that the sEMG signals are related to human joint torques and occur prior to the execution of movement [24]. Since this sensing solution may result in a very intuitive usage, sEMG signals have been successfully employed in most of the exoskeleton robots for rehabilitation and assistive purposes. However, sEMG sensors have practical limitations such as subject dependence, sensitivity to the sensing location, low signal-to-noise-ratio, and low repeatability, which do not make them robust enough for daily usage.

A more common and robust method consists in extracting the human intention from the subject's movements, through position sensors, or with force/torque sensors at the human-robot interface. These can then be combined with an impedance/admittance control scheme and a dynamic model of the human limbs [25–27]; the robot can then deliver the appropriate assistance level to compensate for the user's lack of muscular strength. The main advantage of this approach is that it can shape a virtual (or desired) impedance while keeping the patient engaged in the task, allowing to assess his/her movement ability and guaranteeing a safe interaction [28].

In this section, we assume that the robot used for rehabilitation/assistance has a fixed mechanical impedance. The sensing control strategy is addressed using the impedance/admittance paradigm to set the desired stiffness or damping, providing the assistance effort required.

MECHANICAL IMPEDANCE/ADMITTANCE CONTROL

Mechanical impedance is the relationship between the net force applied on a mechanical system and the system's resulting kinematics, that is, position, velocity, and acceleration [29]. If the system is linear and time invariant, the impedance of the system can be expressed in the Laplace domain as the second-order transfer function $Z(s)$ relating the net force $F(s)$ to the position $X(s)$ as in Eq. (1):

$$Z(s) = \frac{F(s)}{X(s)} = Ms^2 + Bs + K \tag{1}$$

where the parameters M, B, and K denote, respectively, the mass, damping coefficient, and stiffness of the system, that is, the coupled system formed by the robot and the human limb. The terms M, B, and K represent the physical mechanical properties of the coupled system, which are passive and constant. Under the robot's control and actuator force $F_a(s)$, the actual dynamic behavior of the system can be modified and replaced by a set of virtual (or desired) parameters M_d, B_d, and K_d. This form of control is referred to as the impedance/admittance control.

Shaping the desired mechanical impedance not only effectively provides an assistance but also allows the user to safely interact with the robot. In addition to the

acting force $F(s)$, the system is subject to the actuator effort $F_a(s)$ generated by the motor. The impedance/admittance control can adjust the actuator's force $F_a(s)$ such that the user feels a different impedance, defined in Eq. (2):

$$Z_d(s) = M_d s^2 + B_d s + K_d \tag{2}$$

where the terms M_d, B_d, and K_d represent, respectively, the desired mass, desired damping coefficient, and desired stiffness. The implementation of a compliant controller can be accomplished in two ways, usually referred to as indirect force control strategies: impedance-based force generator and admittance-based trajectory generator.

Although various alternatives have been proposed for these two schemes, we will herein focus only on their most general implementations, that is, the closed-loop impedance and admittance schemes, which rely on the feedback from both a position and on a force sensor, and the open-loop variation of the impedance control, which has found broad application in rehabilitation robotics.

Impedance control

The goal of impedance control is to define the desired impedance between a desired input position $X_d(s)$ and the actuator force $F_a(s)$. The impedance control comprises an inner force control loop $F_s(s)$ and an outer position feedback loop with a position sensor [30]. The control diagram is illustrated in Fig. 3B.

The measured position $X(s)$ is used as an input to an impedance control containing the desired impedance parameters in the form $Z_d(s)$. The impedance control generates a desired force $F_d(s)$ as in Eq. (3). The desired actuator force $F_d(s)$ and the actual kinematic trajectory $X(s)$ are used to control the robot through the inner force control loop. As a result, the robot executes the command and applies an assistive force $F_a(s)$ on the user to perform the desired motion:

$$F_d(s) = \left(M_d s^2 + B_d s + K_d\right)\left[X_d(s) - X(s)\right] \tag{3}$$

where $X_d(s)$ is the desired position of the system.

The issue of the impedance control is related to the high-performance requirement for the inner force control loop. Depending on the coupled system dynamics, a low gain for the force control can cause inferior performance, whereas a high gain tuning can lead to instability.

The open-loop version of impedance control avoids stability issues in the inner force loop by removing the feedback from the force sensor. This implementation practically translates in an outer position loop the implements the desired impedance and delivers forces through the motor in current mode. Note that such framework requires the actuator to be backdrivable, relies on accurate modeling of the robot's dynamics, and is not suitable to render high impedances.

Admittance control

The admittance control scheme comprises an admittance-based trajectory generator and a force sensor in a feedback loop. The admittance control scheme shown in Fig. 3C is a common solution to guarantee *backdrivability by control* when nonbackdrivable actuators are used.

The huge advantage of the admittance control is its robustness thanks to the inner position control $P_c(s)$, the objective of the inner control loop is to accurately track the desired trajectory $X_d(s)$ as fast as possible, while the outer force loop is responsible for modifying the force-position relation (4) [30]:

$$X_d(s) = \frac{F(s)}{Z_d(s)} = \frac{F(s)}{M_d s^2 + B_d s + K_d} \tag{4}$$

where the outer force loop computes the desired motion $X_d(s)$ when the acting force $F(s)$ is sensed based on the desired impedance parameters. Thus, the admittance control paradigm is the preferred approach, showing considerable advantages, for applications requiring large stiffness (such as haptic devices) or exoskeleton robots with nonbackdrivable actuators [31]. The main drawback of the admittance control arises when a low impedance is desired. This is because a low desired impedance implies high desired admittance, which may result in instability. A further limitation is inaccurate impedance-rendering due to the imprecise inner position control loop; this can be caused by numerous factors, among which nonlinear phenomena such as friction and backlash play a key role.

FRICTION AND BACKLASH COMPENSATION

All mechanical systems, independently of the nature of their actuation stage and transmission components, and no matter how well designed, will exhibit some degree of unwanted friction and backlash. These phenomena, deriving, respectively, from the interaction between contiguous surfaces and a play between adjacent movable parts, can significantly affect the performance of the device, reducing its tracking accuracy and bandwidth and influencing the stability of a closed-loop controller [32]. Addressing these issues is particularly relevant when one requires accurate position controlling or force rendering and in applications, such as rehabilitation robotics, where safety in the human-robot interaction is of paramount importance.

When the effect of backlash and friction is significant, it leads to nonlinear behaviors such as stick-slip and hysteresis, making common linear control strategies such as proportional-integrative-derivative (PID) unsuitable to meet the application's requirements. More elaborate controllers thus need to be designed, including a model or a strategy that accounts and compensates for the effects of nonlinearities [33].

If a sufficiently accurate mathematical description of the system is available, the essence of compensation comes down to using a feedforward command that is equal and opposite to the instantaneous force/position deficit caused by friction and backlash, respectively. This has resulted in a rich and varied literature on modeling nonlinear systems with complex dynamics [34,35]. Alternatively, one could use a strategy that is not based on any model for counteracting unwanted effects, by opportunely choosing the control gain parameters or using nonmodel-based observers [36].

In this section, we'll review the most common model-based strategies adopted to control mechanical systems with friction and backlash, focusing on the mathematical formalisms developed to describe these phenomena and on their practical usage.

FRICTION

Although friction may be a desirable property, it is often an impediment for servo control. Tribology, that is, the science of rubbing contacts, has produced a vast variety of descriptive mathematical tools that can be exploited when controlling systems with friction. This section is by no means complete and will only touch on some of the most common and practical approaches for engineering. An elegant and exhaustive review of such tools can be found in Armstrong-Helouvry et al. [35].

The first known studies on the science of rubbing contact surprisingly date back to the pre-Newtonian era, when Leonardo da Vinci first recognized friction as being a force proportional to the load, opposed to motion and independent of contact area [29]. After the elucidation of Newton's first law, da Vinci's model was formalized by, among others, Amonton and Coulomb [37,38]. The Coulomb model for friction is widely used for its simplicity and can easily be formalized as an ideal relay:

$$F = F_c sgn(v) \tag{5}$$

$$F_c = \mu F_N \tag{6}$$

with μ being a constant friction coefficient, F_N the normal load and $sgn(v)$ the sign function of the velocity.

In 1833, Morin introduced the idea of static friction [39] that was later combined with the viscous models introduced by Reynolds [40], resulting in one of the most commonly used friction models in engineering, shown in Fig. 4A. The model incorporates the concept of static friction (or stiction), that is, friction at zero velocity, breakaway force, that is, the force required to overcome the stiction, and the velocity-dependent nature of friction for nonzero velocities. A common formalization of this model takes the form

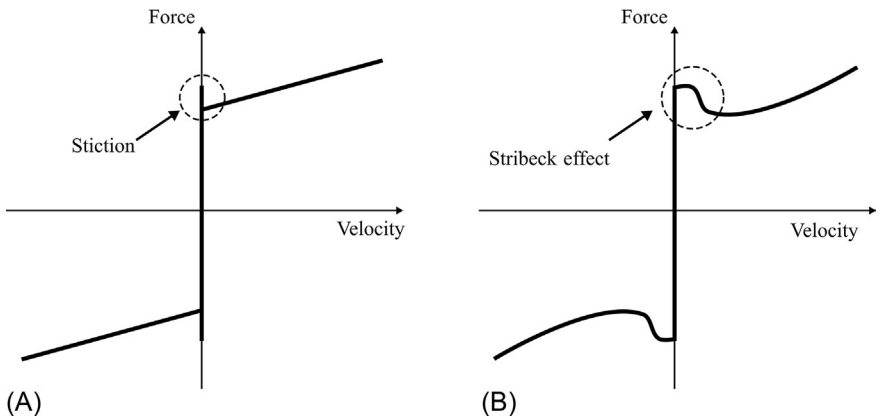

FIG. 4

Static friction and Stribeck effect. (A) Stiction model with viscous friction. (B) Stiction model with Stribeck effect and viscous friction.

$$F = \begin{cases} F_e & \text{if } v = 0 \text{ and } |F_e| < F_s \\ F_s \, sgn(F_e) & \text{if } v = 0 \text{ and } |F_e| \geq F_s \\ \beta v & \text{if } v \neq 0 \end{cases} \tag{7}$$

with F_e being an external force, F_s the breakaway force, and beta a viscous coefficient.

Stribeck [41] later observed that the drop in force at the initiation of motion is not a discontinuous function but depends on the velocity:

$$F = \begin{cases} F_e & \text{if } v = 0 \text{ and } |F_e| < F_s \\ F_s \, sgn(F_e) & \text{if } v = 0 \text{ and } |F_e| \geq F_s \\ F(v) & \text{if } v \neq 0 \end{cases} \tag{8}$$

with $F(v)$ being an arbitrary function for which many parametrizations have been proposed and which may take the form shown in Fig. 4B. A common formalization is

$$F(v) = F_c + (F_s - F_c) e^{-\left|v/v_\sigma\right|^{\delta\sigma}} + \beta v \tag{9}$$

where $F(v)$ is known as the Stribeck velocity and $\delta\sigma$ is a parameter that can be tuned to best fit the shape of the Stribeck effect.

Although widely used for their simplicity, the discontinuities at zero of the previous models make them impractical for friction compensation at motion stop and inversion, where some of the most unwanted effect (e.g., stick-slip) can arise. Dynamic models that include a smooth transition between the two friction regimes instead of a switching function have thus attracted interest from the control community.

Many attractive features for model-based friction compensation have been shown by the LuGre model [42] that is probably the most widely used choice in the research community for both its fidelity in simulating realistic friction behaviors and its ease of implementation. The LuGre model has been used for friction compensation with complex nonlinear systems such as robotic manipulators [42] and wearable assistive devices [27], its simplicity making is suitable for adaptive frameworks.

The underlying reasoning of the LuGre model is not unlike that of the Bristle model: friction derives from the deflection of bristles at the contact points of the moving surfaces. Friction force is a function of the bristles' average deflection, described by a state variable z:

$$\dot{z} = v - \frac{|v|}{g(v)} \sigma_0 z \tag{10}$$

$$F = \sigma_0 z + \sigma_1 \dot{z} + f(v) \tag{11}$$

where σ_0 and σ_1 are constant parameters and $g(v)$ and $f(v)$ model the Stribeck effect and the viscous friction, respectively. The most common choices for these two functions are those that result in a steady-state force similar to Eq. (9):

$$g(v) = \alpha_0 + \alpha_1 e^{-\left(v/v_0\right)^2} \tag{12}$$

$$f(v) = \alpha_2 v \tag{13}$$

with α_i and v_0 being coefficients determining the characteristics of the friction curve such as the stiction force and the Stribeck effect's profile.

Details about other parametrizations for $g(v)$ and $f(v)$ and about identification procedures for the LuGre model can be found in [43]. Once a good model of friction in the robot is available, friction can be predicted and compensated using a feedforward term in the control block.

BACKLASH

Backlash is present in any mechanical system where the driving member is not directly connected to the load. The most common case occurs with gears, where the loss of contact between teeth at motion inversion causes a backlash gap to open. When this occurs, the load is uncoupled from the motor, and the actuator's torque drives only the components before the backlash. This can result in a significant deterioration of motion control and, in the worst case, in loss of stability.

Some of the most important developments in control of systems with backlash was pioneered by Tao and Kokotovic [44], who proposed to use an inversion of the backlash nonlinearity in the control to cancel out the physical phenomenon. Since backlash causes position hysteresis, useful tools for identification and control have been proposed from the extensively researched field of hysteresis modeling.

Several mathematical formalisms exist for modeling backlash-induced hysteresis, but the Bouc-Wen model has been proven to capture a wide range of hysteresis phenomena while retaining a low level of complexity and computational effort and has been successfully used for accurate position control of wearable robotic devices [45].

The Bouc-Wen model represents the hysteresis cycle using a mapping between an input variable $x(t)$ and an output $y(x,t)$ using an auxiliary state variable z:

$$y(x,t) = \alpha k x(t) + (1-\alpha) D k z(t) \tag{14}$$

$$\dot{z} = D^{-1}\left(A\dot{x} - \beta|\dot{x}||z|^{n-1} z - \gamma\dot{x}|z|^n\right) \tag{15}$$

with $n \geq 1$, $D > 0$, $k > 0$, and $\alpha \in 0, 1$. A, β, and γ are dimensionless parameters that can be tuned to control the size and shape of the hysteresis loop and n governs the smoothness of the transition between the elastic and plastic response. Note that the output is given by the sum of a purely elastic term ($kx(t)$) and a hysteretic contribution ($Dkz(t)$), with α controlling the weight of each on the output.

Identification strategies for the model's parameters include least mean square, genetic algorithms, particle swarm optimization, and neural networks. The feedforward term, deriving from the model, can be used in an open-loop scheme alone, combined with a feedback term or combined with feedback information for continuous adaptation.

IMPLICATIONS FOR THE CONTROL OF REHABILITATION ROBOTS

One of the most profound engineering challenges in designing robots for rehabilitation is achieving the dual goal of delivering high forces while retaining the backdrivability of the device. Backdrivability has been shown to be a fundamental feature for keeping the patient engaged in the task, for assessing his/her movement ability and for guaranteeing the system's safety. Yet the requirements of minimizing the intrinsic dynamics on one hand and providing high force output on the other are at odds since the latter requires bulkier actuators or reduced transmissions, which compromise the efficiency of the system and reduce its dynamic transparency.

For stationary robots, where portability is not paramount or devices that need not render extremely high forces, using larger actuators in a direct drive (or small reduction) configuration is probably the most convenient choice. The absence of complex transmission mechanisms will not diminish the efficiency of the motor, allowing it to be back-driven. For such systems, one could implement an open-loop impedance controller, well-known for its stability, simply using the position sensors on the motors' axes. Modeling the robot's dynamics and compensating for backlash and hysteresis is, here, critical.

A device designed for portability or for rendering high impedances, on the other hand, will most likely require a highly reduced and thus nonbackdrivable transmission. An open-loop impedance control in this configuration becomes unfeasible, and a force sensor between the device and the subject is needed to monitor the interaction forces and achieve backdrivability by control. Both the closed-loop impedance and admittance controllers are viable options, but the former is more prone to stability issues, while the latter is robust thanks to the inner position control loop. The drawback of admittance controllers, that is, low accuracy, can be dealt with through accurate identification and compensation of nonlinear phenomena that could upset the inner position feedback loop, for example, friction and backlash in the transmission.

Finally, a significant advantage in terms of intrinsic safety, low-cost force measurement by spring displacement and, most of all, increased force control robustness can be achieved using SEAs. The drawback is the compulsory need for force sensing between the robot and the subject.

CONCLUSION

In this chapter, we gave an overview of the most commonly used actuation strategies for rehabilitation robots, where the characteristics of the interaction between the robot and its user play a key role. Being electric actuators the most commonly employed solution, we briefly described the two frameworks used to achieve compliant control with DC motors.

Both frameworks require compensation of nonlinear phenomena, such as friction and backlash, to ensure stability and accurate force rendering; we gave the reader

an overview of what we believe to be the most practical and effective tools to compensate for such phenomena. Finally, the last section explores the difficult trade-off between high force rendering and backdrivability in rehabilitation robots.

REFERENCES

[1] Feigin VL, Roth GA, Naghavi M, Parmar P, Krishnamurthi R, Chugh S, et al. Global burden of stroke and risk factors in 188 countries, during 1990–2013: a systematic analysis for the Global Burden of Disease Study 2013. Lancet Neurol 2016;15(9):913–24.

[2] Go AS, Mozaffarian D, Roger VL, Benjamin EJ, Berry JD, Blaha MJ, et al. Heart disease and stroke statistics—2014 update: a report from the American Heart Association. Circulation 2014;129(3):e28–292.

[3] Kwakkel G, Kollen B, Lindeman E. Understanding the pattern of functional recovery after stroke: facts and theories. Restor Neurol Neurosci 2004;22(3–5):281–99.

[4] Igo Krebs H, Hogan N, Aisen ML, Volpe BT. Robot-aided neurorehabilitation. IEEE Trans Rehabil Eng 1998;6(1):75–87.

[5] A Hussain, A Budhota, CML Hughes, WD Dailey, DA Vishwanath, CWK Kuah, et al., Self-paced reaching after stroke: a quantitative assessment of longitudinal and directional sensitivity using the H-man planar robot for upper limb neurorehabilitation Front Neurosci, vol. 10, no. OCT, 2016.

[6] Maciejasz P, Eschweiler J, Gerlach-Hahn K, Jansen-Troy A, Leonhardt S. A survey on robotic devices for upper limb rehabilitation. J Neuroeng Rehabil 2014;11(1):3.

[7] Dovat L, Lambercy O, Gassert R, Maeder T, Milner T, Leong TC, et al. HandCARE: A cable-actuated rehabilitation system to train hand function after stroke. IEEE Trans Neural Syst Rehabil Eng 2008;16(6):582–91.

[8] Hassani V, Tjahjowidodo T, Do T. A survey on hysteresis modeling, identification and control. Mech Sys Signal 2014;49(1–2):209–33.

[9] Gopura RARC, Bandara DSV, Kiguchi K, Mann GKI. Developments in hardware systems of active upper-limb exoskeleton robots: a review. Rob Auton Syst 2016;75:203–20.

[10] Dollar AM, Herr H. Lower extremity exoskeletons and active orthoses: challenges and state-of-the-art. IEEE Trans Robot 2008;24(1):144–58.

[11] Jarrassé N, Morel G. Connecting a human limb to an exoskeleton. IEEE Trans Robot 2012;28(3):697–709.

[12] Mao Y, Agrawal SK. Design of a cable-driven arm exoskeleton (CAREX) for neural rehabilitation. IEEE Trans Robot 2012;28(4):922–31.

[13] Marchal-Crespo L, Reinkensmeyer DJ. Review of control strategies for robotic movement training after neurologic injury. J Neuroeng Rehabil 2009;6(1):20.

[14] Tsagarakis NG, Caldwell DG. Development and control of a 'soft-actuated' exoskeleton for use in physiotherapy and training. Auton Robots 2003;15(1):21–33.

[15] Yap HK, Khin PM, Koh TH, Sun Y, Liang X, Lim JH, et al. A fully fabric-based bidirectional soft robotic glove for assistance and rehabilitation of hand impaired patients. IEEE Robot Autom Lett 2017;2(3):1383–90.

[16] Noritsugu T, Tanaka T. Application of rubber artificial muscle manipulator as a rehabilitation robot. IEEE/ASME Trans Mech 1997;2(4):259–67.

[17] Pratt GA, Williamson MM. In: Series elastic actuators. IEEE/RSJ international conference on intelligent robots and systems. Human robot interaction and cooperative robots, vol. 1, no. 1524; 1995. p. 399–406.

[18] Bicchi A, Peshkin MA, Colgate JE. Safety for physical human-robot interaction. In: Siciliano B, Khatib O, editors. Springer handbook of robotics. Berlin: Springer; 2008. p. 1335–48.
[19] S Eppinger and W Seering, "Understanding bandwidth limitations in robot force control," 1987 Proceedings IEEE Int. Conf. Robot. Autom., vol. 4, 904–909, 1987.
[20] Veneman JF, Kruidhof R, Hekman EEG, Ekkelenkamp R, Van Asseldonk EHF, Van Der Kooij H. Design and evaluation of the LOPES exoskeleton robot for interactive gait rehabilitation. IEEE Trans Neural Syst Rehabil Eng 2007;15(1):379–86.
[21] Westlake KP, Patten C. Pilot study of Lokomat versus manual-assisted treadmill training for locomotor recovery post-stroke. J Neuroeng Rehabil 2009;6(1):18.
[22] Kazerooni H, Steger R, Huang L. Hybrid control of the berkeley lower extremity exoskeleton (BLEEX). Int J Rob Res 2006;25(5–6):561–73.
[23] Kong K, Tomizuka M. Control of exoskeletons inspired by fictitious gain in human model. IEEE/ASME Trans Mech 2009;14(6):689–98.
[24] Farina D, Member S, Jiang N, Rehbaum H, Member S. The extraction of neural information from the surface emg for the control of upper-limb prostheses: emerging avenues and challenges. IEEE Trans Neural Syst Rehabil Eng 2014;22(4):797–809.
[25] Hogan N. In: Impedance control: an approach to manipulation. Am. Control Conf. 1984 IS—SN—VO, no. March; 1985. p. 304–13.
[26] Aguirre-Ollinger G, Colgate JE, Peshkin MA, Goswami A. Active-impedance control of a lower-limb assistive exoskeleton. In: 2007 IEEE 10th international conference on rehabilitation robotics, ICORR'07. 2007. p. 188–95.
[27] Dinh BK, Xiloyannis M, Antuvan CW, Cappello L, Masia L. Hierarchical cascade controller for assistance modulation in a soft wearable arm exoskeleton. IEEE Robot Autom Lett 2017;2(3):1.
[28] Volpe B, Krebs H, Hogan N, Edelstein L, Diels C, Aisen M. A novel approach to stroke rehabilitation: robot aided sensorimotor stimulation. Neurology 2000;54(10):1938.
[29] Leonardo DV. The notebooks. New York: Dover Publications Inc; 1883.
[30] Calanca A, Muradore R, Fiorini P. A review of algorithms for compliant control of stiff and fixed-compliance robots. IEEE/ASME Trans Mech 2016;21(2):613–24.
[31] Kern TA. Engineering haptic devices. 2009, Springer.
[32] Tustin A. The effects of backlash and of speed-dependent friction on the stability of closed-cycle control systems. J Inst Electr Eng—Part IIA Autom Regul Servo Mech 1947;94(1):143–51.
[33] Adams J, Payandeh S. On methods for low velocity friction compensation: theory and experimental study. J Robotic Syst 1996;13:391–404.
[34] Krasnoselskii MA, Pokrovskii AV. Systems with hysteresis. Springer; 1989.
[35] Armstrong-Helouvry B, Dupont P, De Wit CC. A survey of models, analysis tools and compensation methods for the control of machines with friction. Automatica 1994;30(7):1083–138.
[36] Armstrong B, Neevel D, Kusik T. New results in NPID control: tracking, integral control, friction compensation and experimental results. IEEE Trans Control Syst Technol 2001;9(2):399–406.
[37] Amonton G. On the resistance originating in machines. Proc French R Acad Sci A 1699;206–22.
[38] Coulomb C. Théorie Des Machines Simples, En Ayant Egard au Frottement De Leurs Parties, et a la Roideur Des Cordages. Mém Math 1785;.

[39] Morin AJ. New friction experiments carried out at Metz in 1831–1833 [in French]. Mémoires L'Académie R des Sci 1833;4:1–128. 591–696.
[40] Reynolds O. On the theory of lubrication and its application to Mr. Beauchamp tower's experiments, including an experimental determination of the viscosity of olive oil. Philos Trans R Soc Lond A 1886;177:157–234.
[41] Stribeck R. The key qualities of sliding and roller bearings. Zeitschrift Des Vereins Dtsch Ingenieure 1902;46:1342–8.
[42] Canudas de Wit C, Olsson H, Astrom KJ, Lischinsky P. A new model for control of systems with friction. IEEE Trans Automat Contr 1995;40(3):419–25.
[43] de Witt CC, Lischinsky P. In: Adaptive friction compensation with dynamic friction model. Proc. 13th IFAC triennial world congress; 1996.
[44] Tao G, Kokotovic P. Adaptive control of systems with sensor and actuator nonlinearities. Wiley; 1996, 294.
[45] BK Dinh, L Cappello, M Xiloyannis, and L Masia, "Position control using adaptive backlash compensation for bowden cable transmission in soft wearable exoskeleton," in IEEE international conference on intelligent robots and systems, 2016, vol. 2016–Novem.